References

Berry, L., 1984. Desertification in the Sudano–Sahelian region, 1977–1984. Desertification Control Bulletin 10, UNEP.

Berz, G., 1993. The insurance industry and IDNDR: common interests and tasks. IDNDR Newsletter, #15, Osservatorio Vesuviano, pp. 8–11.

Bruce, J.P., 1993. Natural disasters and global change. IDNDR Newsletter #15, Osservatorio Vesuviano, p. 3.

Bottorff, H., 1994. Rapid relief: GPS helps assess Mississippi River flood damage. GPS World, 5(5): 22–28.

Coleman, J.M., 1969. Brahmaputra River: channel processes and sedimentation. Sediment. Geol., 3: 129–239.

Cooke, R.U. and Reeves, R.W., 1976. Arroyos and Environmental Change in the American South-West. Clarendon Press, Oxford, 276 pp.

Defense Mapping Agency, 1992. Digital Chart of the World. Washington, 6 compact disks.

Demek, J., 1972. Manual of Detailed Geomorphological Mapping. IGU Commission on Geomorphological Survey and Mapping, Prague, 344 pp.

Evans, D.M., 1966. Man-made earthquakes in Denver. Geotimes, 10: 11–18.

Harrold, L.L., 1971. Effects of vegetation on storm hydrographs. In: Biological Effects in the Hydrological Cycle. 3rd Intl. Seminar for Hydrology Professors, NSF, pp. 332–346.

Hively, W., 1988. Global Change. Am. Sci., 76(2): 127–130.

Huh, O.K., Ali, A. and Quadir, D.A., 1985. Use of NOAA satellite AVHRR data to monitor river flood hydrology in Bangladesh. Report to UNFAO, Louisiana State University, 36 pp.

Islam, M., 1990. Environmental Perceptions and Agriculture: Environmental Aspects of Agricultural Development in Bangladesh. University Press, Dhaka, 321 pp.

Kahn, A.R. and Nazem, N.I., 1988. Abundance and scaricty of water in Bangladesh: Issues revisited. BIISS J., 9(4).

Kaith, D.C., 1960. Forest practices in control of avalanches, floods, and soil erosion in the Himalayan Front. Proc. Fifth World Forestry Congr., Seattle (3): 1640–1643.

Kubo, S., 1993. Geomorphological features of northwestern Bangladesh and some problems on flood mitigation. GeoJournal, 31(4): 313–318.

Lohmann, E., 1993. Strategy design and policy making for extreme weather events as a result of climatic changes. IDNDR Newsletter #15, Osservatorio Vesuviano, pp. 6–10.

Meyers, M.F. and White, G.F., 1993. Floods... and floods of studies. Nat. Hazards Observer, 18(2): 1–2.

National Academy of Sciences, 1987. Confronting Natural Disasters. National Academy Press, 60 pp.

Office of Technology Assessment, 1993. Preparing for an Uncertain Climate. GPO, 2 Vols., 768 pp.

Pearson, M.L. and Oliver, J.G., 1992. Reconnaissance report: flooding resulting from typhoon Uring in Ormoc City, the Philippines. Waterways Experiment Station, Misc. Paper GL-92, Corps of Engineers, Washington, 49 pp.

Penmetrics, Inc., 1993. Fact sheet on pen-based computers with integral GPS capabilities. Unpub. Memorandum, Corvallis, 2 pp.

Rasid, H. and Pramanik, M., 1990. Visual interpretation of satellite imagery for monitoring floods in Bangladesh. Environ. Manage., 14(6): 815–821.

Reynolds, W., 1990. Personal communication concerning Corps of Engineers study of groundwater availability in Pacific atolls due to sea-level rise.

Rosenfeld, C.L., 1980. Observations on the Mount St. Helens eruption. Am. Sci., 68(5): 494–509.

Rosenfeld, C., 1984. Remote sensing for geomorphologists. In: J. Costa and P. Fleisher (Editors), Developments and Applications of Geomorphology. Springer, Berlin, pp. 1–37.

Rosenfeld, C.L., 1987. Observation and measurement of erossion following the 1980 eruptions of Mount St. Helens, Washington, USA. In: A. Goddard and A. Rapp (Editors), Processus et Mesure de l'Erosion. 25th Int. Geographical Congr., Paris. CNRS, pp. 565–571.

Rosenfeld, C.L., 1992. Watershed management: fighting the effects of drought in west Africa. Geo Info Systems, 2(3): 29–39.

Rosenfeld, C.L., 1994. Flood hazard reduction: GIS maps survival strategies in Bangla Desh. Geo Info Syst., 4(5): 30–37.

Rosenfeld, C. and Pearson, M., 1982. Aerial monitoring of the erosional characteristics of the North Fork Toutle River: a geomorphic approach to sediment yield. Final Report, Portland District, Corps of Engineers, 99 pp.

Simpkin, T., Seibert, T., McClelland, L., Bridge, D., Newhall, C., Latter, J., 1981. Volcanoes of the World. Hutchinson-Ross, Stroudsburg, 233 pp.

Schweig, E.S., 1994. A wake-up call from Northridge. Nat. Hazards Observer, 18(4): 2–3.

Swanson, F.J. and Dyrness, C.T., 1975. Impact of clearcutting and road construction on soil erosion by landslides in the western Cascade Range, Oregon. Geology, 3: 494–496.

Tricart, J., 1965. Principes et Méthodes de la Géomorphologie. Legende des Cartes Géomorphologique. Masson, Paris, pp. 185–242.

Tweedie, A., 1966. Water and the World. Nelson, Sidney, 317 pp.

UNESCO, 1963. Changes of Climate. Arid Zone Research, Vol. 20, UNESCO, Paris, 488 pp.

Verstappen, H.Th., 1993. The International Decade for Natural Disaster Reduction and the IGU flood hazard research programme. GeoJournal, 34(4): 309–312.

Verstappen, H. and Van Zuidam, R., 1989. The ITC system of geomorphologic survey. Int. Inst. for Aerospace Survey and Earth Sciences (ITC), Enschede, 41 pp.

Watari, M. (Editor), 1988. Landslides in Japan. Nat. Conf. on Landslide Control. Japan Society of Landslides, 54 pp.

ELSEVIER

Geomorphology 10 (1994) 37–63

GEOMORPHOLOGY

Geologic effects of hurricanes

Nicholas K. Coch

Geology Department, Queens College, CUNY, Flushing, NY 11367, USA

Received February 10, 1994; revised March 27, 1994; accepted April 2, 1994

Abstract

Hurricanes are intense low pressure systems of tropical origin. Hurricane damage results from storm surge, wind, and inland flooding from heavy rainfall. Field observations and remote sensing of recent major hurricanes such as Hugo (1989), Andrew (1992) and Iniki (1992) are providing new insights into the mechanisms producing damage in these major storms. Velocities associated with hurricanes include the counterclockwise vortex winds flowing around the eye and the much slower regional winds that steer the hurricane and move it forward. Vectorial addition of these two winds on the right side of the storm gives a higher effective wind speed than on the left side. Coast-parallel hurricane tracks keep the weaker left side of the storm against the coast, whereas coast-normal tracks produce a wide swath of destruction as the more powerful right side of the storm cuts a swath of destruction hundreds of kilometers inland. Storm surge is a function of the wind speed, central pressure, shelf slope, shoreline configuration, and anthropogenic alterations to the shoreline. Maximum surge heights are not under the eye of the hurricane, where the pressure is lowest, but on the right side of the eye at the radius of maximum winds, where the winds are strongest. Flood surge occurs as the hurricane approaches land and drives coastal waters, and superimposed waves, across the shore. Ebb surge occurs when impounded surface water flows seaward as the storm moves inland. Flood and ebb surge damage have been greatly increased in recent hurricanes as a result of anthropogenic changes along the shoreline.

Hurricane wind damage occurs on three scales — megascale, mesoscale and microscale. Local wind damage is a function of wind speed, exposure and structural resistance to velocity pressure, wind drag and flying debris. Localized extreme damage is caused by gusts that can locally exceed sustained winds by a factor of two in areas where there is strong convective activity.

Geologic changes occurring in hurricanes include beach erosion, dune erosion, inlet formation from flood and ebb surge, landscape changes through tree destruction by wind and nearshore channeling and sedimentation resulting from ebb surge.

Multi-decadal wet and dry cycles in West Africa seem to be associated with increases (wet periods) and decreases (dry periods) in the frequency of Atlantic Coast landfalling hurricanes. Coastal zone population and development has increased markedly in a time of low hurricane frequency in the 24 year dry cycle from 1970 to the present. However, no previous climatic cycle in this century has exceeded 26 years. We may be entering a multi-decadal cycle of greater hurricane activity, placing these highly urbanized shorelines in considerable danger.

1. Introduction

Hurricanes Hugo (1989) in South Carolina, Andrew (1992) in South Florida, and Iniki (1992) in Hawaii have provided valuable insights into the geologic processes and damage patterns associated with major storms. New technological advances such as satellite imaging, computer simulation and prediction of storm surge, and Doppler Radar analysis of approaching storms have yielded new data useful in analyzing damage intensities and types. In addition, analysis of these storms have been increasingly interdisciplinary with meteorologists as well as geologists, biologists, engi-

SSDI 0169-555X(94)00016-K

639

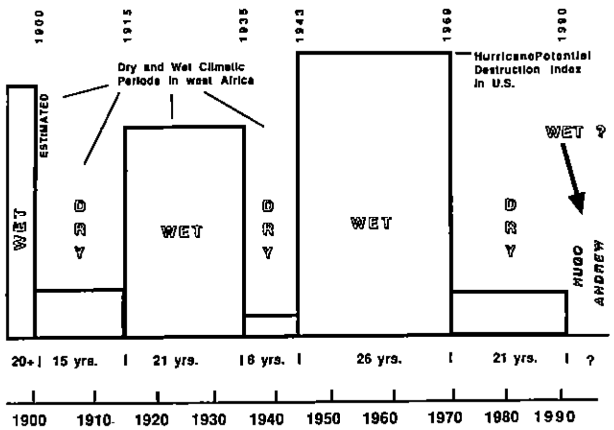

Fig. 1. Hurricane damage potential related to multi-decadal wet and dry cycles in West Africa. The hurricane damage potential (vertical scale of diagram) is a measure of a hurricane's potential for wind and storm surge destruction. It is defined as the sum of the square of a hurricanes maximum wind speed (in 10^4 knots^2) for each 6-hour period of a storm's existence. (After Gray and Landsea, 1991.)

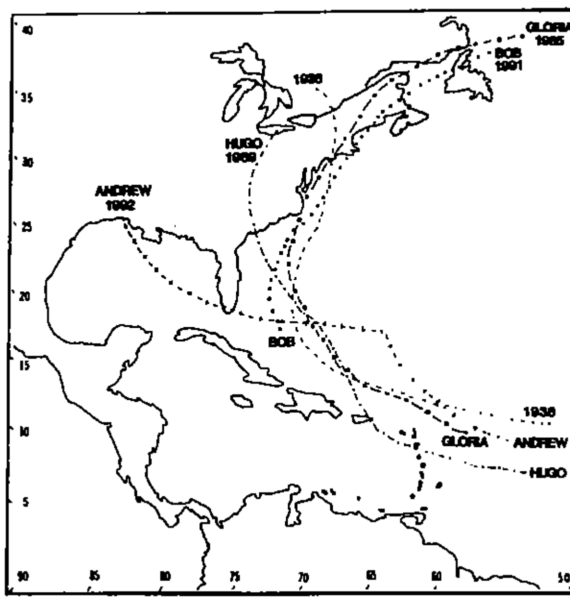

Fig. 2. Map of tracks of hurricanes described in the text.

neers, and emergency managers providing a *holistic* picture of hurricane effects for the first time.

Gray (1990) has shown that the frequency of Atlantic Coast landfalling hurricanes is related to multi-decadal "wet" and "dry" cycles in West Africa. Gray and Landsea (1991) have delineated these wet and dry cycles and the hurricane damage done during each of them for the last century (Fig. 1). During wet cycles, such as 1945–1969 (Fig. 1), Atlantic Coast landfalling hurricanes were more frequent. In contrast, during dry cycles (1970–to ?present) they have been less frequent (Fig. 1). Unfortunately, much of our coastal development has occurred in the 24 years since 1970 when few major hurricanes hit the Atlantic Coast of the United States. This period of relative quiescence has done little to raise hurricane consciousness among coastal inhabitants. No previous wet or dry cycle in this century has lasted more than 26 years (Fig. 1), and many experts believe we soon will be entering a new "wet cycle" in which greater numbers of hurricanes will wreak catastrophic damage on our highly populated and developed shorelines.

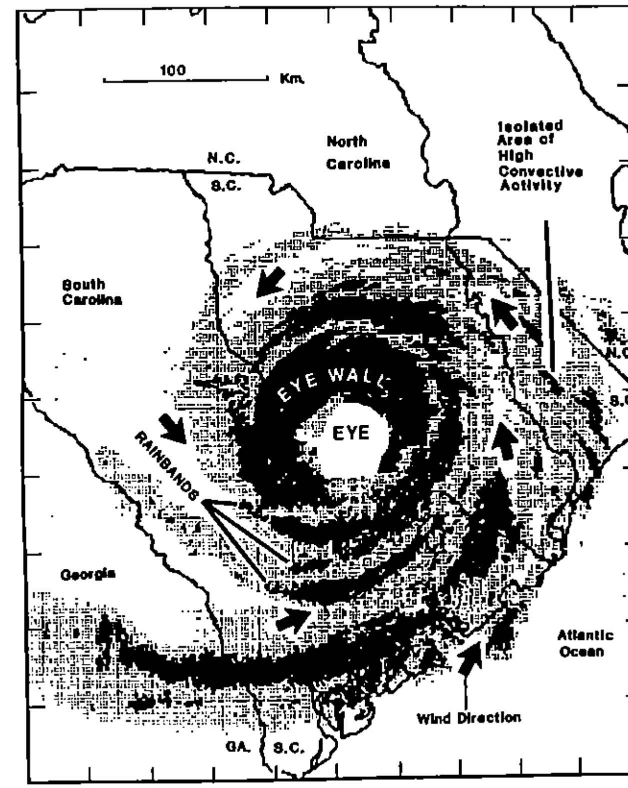

Fig. 3. Doppler Radar image of Hurricane Hugo (1989) showing storm components mentioned in the text. Modified from radar image by Hurricane Research Division, NOAA.

Table 1
The Saffir–Simpson scale for classification of hurricanes based on their wind speeds and storm surge. Some examples of typical damage for each category are included here. Actual damage patterns depend not only on wind speed and surge levels but other factors described in the text. NOAA version of scale (1990)

Category	Wind velocity		Surge height[a,b]		Damage
	(km/h)	(mi/h)	(m)	(ft)	
1	119–153	74–95	1.2–1.5	4–5	No real damage to building structures. Damage primarily to unanchored mobile homes, shrubbery and trees. Also, some coastal road flooding and minor pier damage
2	154–177	96–110	1.8–2.4	6–8	Some roofing material, door and window damage to buildings. Coastal and lowlying escape routes flood 2–4 hours before arrival of center. Small craft in unprotected anchorages break moorings
3	178–209	111–130	2.7–3.6	9–12	Some structural damage to small residences and utility buildings with a minor amount of curtainwall failures. Mobile homes are destroyed. Flooding near the coast destroys smaller structures with larger structures damaged by floating debris. Terrain continuously lower than 5 feet above sea level may be flooded inland as far as 6 miles
4	210–249	131–155	3.9–5.5	13–18	More extensive curtainwall failures with erosion of beach areas. Major damage to lower floors of structures near the shore. Terrain continuously below 10 feet above sea level may be flooded requiring massive evacuation of residential areas inland as far as 6 miles
5	> 249	> 155	> 5.5	> 18	Complete roof failure on many residences and industrial buildings. Some complete building failures with small utility buildings blown over or away. Major damage to lower floors of all structures located less than 15 feet above sea level and within 500 yards of the shoreline. Massive evacuation of low areas within 5–10 miles of the shoreline may be required

[a]Actual storm surge height will vary depending on local coastal configuration and other factors.
[b]Surge heights given above normal water levels.

This paper describes the styles and intensities of hurricane damage and provides information on the factors that increase damage from wind, storm surge and inland flooding. It is based on both published studies of Hurricane Andrew (1992), Iniki (1992), Bob (1991) and Hugo (1989) plus ground and aerial studies of the damage effects of those storms by the author. The tracks of the hurricanes described in this paper are shown in Fig. 2. Information is synthesized from a number of different cognate fields because a *holistic* view of hurricane damage is essential if we are to minimize loss of life and structural damage in future hurricanes.

2. Hurricanes

United States hurricanes are formed in the warm tropical waters of the North Atlantic, the Caribbean and the eastern Pacific and migrate westward and northward until they make landfall. Details on hurricane formation, intensification and migration are given in the work by Risnychok (1990) and Coch (1994).

2.1. Structure

A mature hurricane consists of a calm central area of low pressure referred to as the eye, surrounded by spiral bands of thunderstorm activity (Fig. 3). Note that the rainbands are not continuous, isolated areas of high convective activity occur in the outer parts of the storm, and the winds flow in a counterclockwise direction around the eye (Fig. 3).

The most violent winds and strongest convective activity occur in the eyewall, the section just outside of the eye (referred to as the eyewall). Maximum winds occur in the right front portion of the eyewall in a zone varying from 32–56 km (20–35 miles) wide in a typical hurricane such as Hugo (Fig. 3).

2.2. Power

Hurricanes are classified based on their sustained wind speeds into 5 categories on the Saffir–Simpson Scale (Simpson, 1974). The wind speeds, central pressures, storm surge and typical damage associated with each category is given in Table 1.

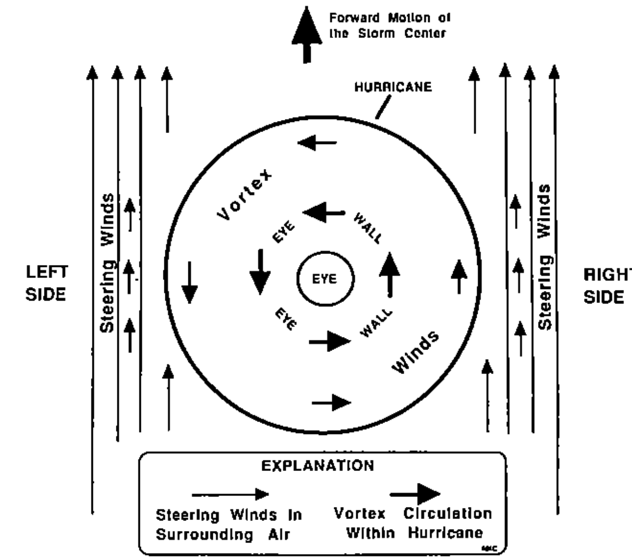

Fig. 4. Diagrammatic view (horizontal section) showing the velocity components described in the text. The high velocity vortex winds flow counterclockwise around the eye. At the same time the storm center is being moved forward by the regional steering winds. Note that on the right side of the storm (looking forward) the two velocities are in the same direction and so are additive. Consequently, the winds on the right side of a hurricane are always stronger.

While the Saffir–Simpson category is defined by sustained wind velocity ranges, other parameters such as the forward velocity of the storm are very important in determining the destructive power of a hurricane. Given two hurricanes of similar power (Saffir–Simpson category), the faster moving one will cause significantly more damage. The regional significance of this is discussed later in this paper.

2.3. Velocity

Two different velocities are associated with hurricanes and their interplay determines the damage intensities and gradients along the diameter of the storm as it makes landfall. The vortex winds are the hurricane force winds (Table 1) that flow counterclockwise around the eye (Fig. 4). The storm system itself, hundreds of kilometers across, is embedded in a regional wind system that guides the storm system forward. This storm center forward velocity is far less than the hurricane force vortex winds flowing around the eye.

The winds on either side of a hurricane are not equal. Note that on the right side of the storm, looking in the direction of movement (Fig. 4) the steering winds and the vortex winds are in the same direction and are thus additive to some degree. On the left side, the winds are in opposite directions and are subtractive. *In short, the winds on the right side of a hurricane are always stronger.*

Forward velocities of hurricane systems also vary with latitude. Southern landfalling hurricanes are under the influence of easterly (trade) wind systems and generally move less than 32 km/h (20 mile/h). Once a hurricane moves northward along the Carolinas, it begins to be affected more by westerly wind systems whose upper level flows are faster. Thus, hurricanes speed up as they move toward the northeastern United States. A more typical speed for a northern hurricane is 48–64 km/h (30–40 mile/h). According to Pierce (1939), the extremely destructive Long Island–New England hurricane (1938) moved forward at a velocity of 97 km/h (60 mile/h).

The northward increase in forward speed of a hurricane has a very important role in increasing damage at, and after landfall. In short, it increases the effective wind on the right side of the storm and this contributes to greater wind damage and the development of a higher storm surge. The increase in speed also affects the power of the storm when it approaches landfall. If a hurricane is moving faster than 56 km/h (35 mile/h) as it passes over the cooler waters south of Long Island, it will not begin to begin to weaken and break up and will release its full power on the land (R. Sheets, pers. commun., 1993). The great forward speed of the 1938

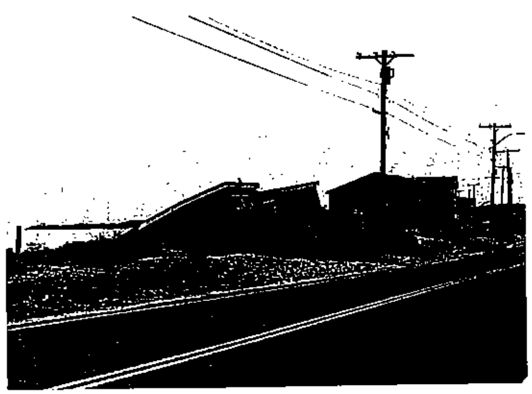

Fig. 5. Hurricane Bob (1991) damage on Cape Cod, Mass. Elevated surge undermined the cottages in the foreground. Note the wind-induced cladding loss on the side of the building (dark area) on the left of the photo. Photograph courtesy of Ana Butler.

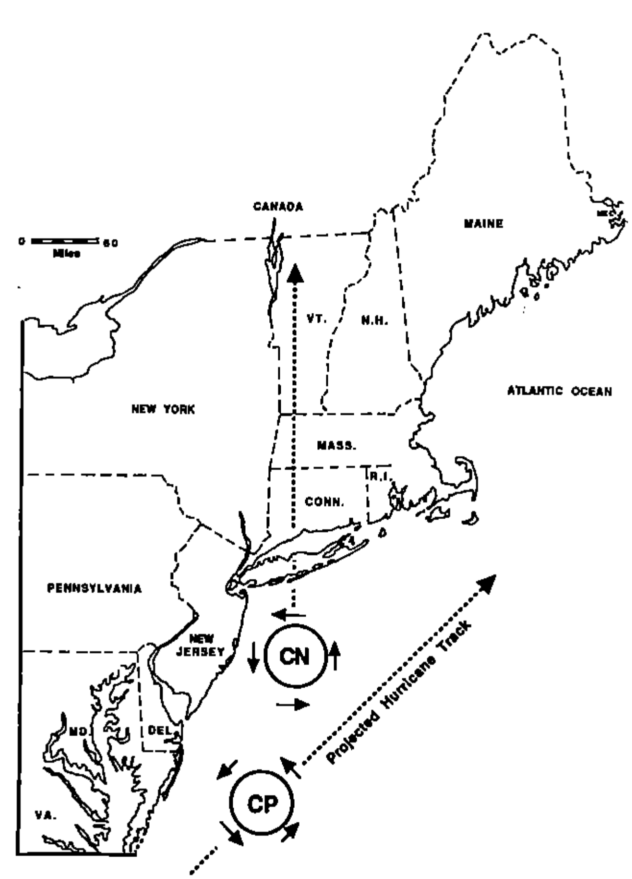

Fig. 6. Tracks of Hurricanes relative to the coastline. In a coast-parallel track (*CP*), the weaker left side of the storm is against the coast. In a coast-normal track (*CN*) the more powerful right side cuts a wide swath of devastation deep inland as it crosses the coast. The problem is especially serious in Long Island and southern new England where most hurricanes have a coast-normal track.

New England Hurricane (Fig. 2) resulted in very little reduction in storm power until it was well into central New England. Hurricane force winds persisted to the Canadian border. In contrast, Hurricane Bob (1991), a potentially dangerous Category 3 hurricane, was moving only 48–56 km/h (30–35 mile/h) as it approached Long Island and southern New England (Fig. 2), and this weakened the storm (Fig. 2). Yet, it still caused considerable destruction in the Cape Cod area of Massachusetts (Fig. 5).

2.4. Tracks

As massive and powerful as a hurricane is (Fig. 3), it is easily blocked by local weather systems and steered by regional upper level wind systems (Coch, 1994). For example, Hurricane Andrew moved steadily northwestward (Fig. 2) until it encountered a high pressure system blocking its northward path and this diverted it sharply westward (Fig. 2) to cut a swath of destruction across South Dade County, Florida. When Andrew moved into the Gulf of Mexico from South Florida, it had a potential northwest track towards the highly developed Texas Coast. However, a low pressure system developed in the western part of the Gulf of Mexico and that prevented the hurricane from drifting westward. The winds associated with that low pressure center steered the hurricane into the relatively unpopulated area of the western Mississippi Delta (Coch, 1994).

One of the most important aspects of hurricane paths is the relationship of the track of the storm to the coastline. In a coast-parallel track (Fig. 6) the storm keeps its weaker left side against the coast and damage drops off rapidly inland. In contrast, in a coast-normal track (Fig. 6) the hurricane crosses the coast and the powerful right side cuts a wide 80–160 km (50–100 miles) swath of heavy destruction deep inland. In the 1938 Long Island–New England Hurricane (Fig. 2), significant damage occurred almost to the Canadian border (Federal Writers Project, 1938). In Hurricane Hugo (Fig. 2) damage extended across South Carolina and deep into North Carolina.

A major hurricane with a coast-normal track striking the highly urbanized northeastern United States could have catastrophic consequences. The path scenario for such a storm is shown in Fig. 7. This meteorological set up occurred in the 1938 Hurricane and in several subsequent hurricanes such as Hurricane Bob (1991). The scenario involves a well developed Bermuda High and a high pressure system moving eastward across the United States. In between the two air masses is a low pressure trough (Fig. 7). This set-up can occur as much as ten times during a hurricane season (from June–October). If the passage of a Category 3 hurricane (Table 1) coincides with such a set up, the hurricane can move around the western edge of the Bermuda High and enter the low pressure trough. It will then speed up as it moves northward and be steered into a heavily developed coast of the northeastern United States with catastrophic consequences (Coch and Wolff, 1990).

It takes only a slight change in hurricane track landfall position to make a great difference in the resulting damage. It is only in the last few hours before landfall that the official forecasts are both accurate and consistent to allow local decision makers to use them as a sure guide to preparatory actions (Carter, 1983). The damage caused by Hurricane Andrew as it made landfall at Homestead, Florida (Fig. 2) was staggering. However, if it had made landfall just 32 km (20 miles) to the north, over the highly developed Miami–Ft. Lauderdale area, the results would have been truly catastrophic.

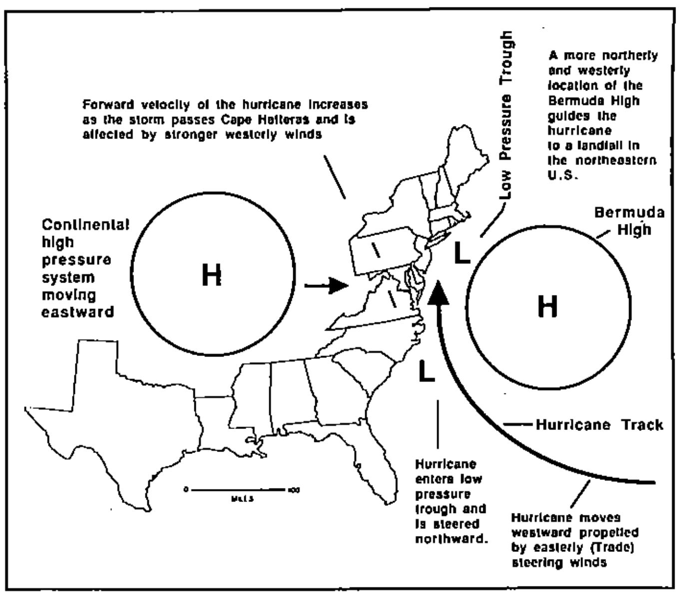

Fig. 7. Meteorological setup favoring landfall of a major hurricane in the northeastern United States. A low pressure zone develops between a continental high and the semi-permanent Bermuda High. If a major hurricane rounds the Bermuda High and enters the low pressure trough, it is directed northward, the storm forward velocity increases as it passes the Carolinas and is affected by stronger upper level westerly winds.

3. Hurricane damage

The damage caused by a hurricane is the sum total of storm surge, wind, and inland flooding caused by high precipitation prior to and during the storm. The wide variety of damage associated with a coast-normal hurricane track crossing a low lying shoreline is shown in generalized fashion in Fig. 8.

The relative percentage of the three types of storm damage at any given locality is a function of three factors: (1) distance from the coast; (2) hurricane side and distance from the eye center and; (3) the strength of isolated conductive activity centers in the outer rainbands (Fig. 3).

Field observations of damage patterns during several recent major hurricanes, as well as remote sensing analysis by governmental agencies during those storms, have provided new insights into the mechanisms which create this damage.

3.1. Storm surge

The elevated sea surface resulting from a storm is referred to as storm surge; this is a topic fraught with misconceptions. People commonly visualize the process as a series of massive tidal waves hitting the coast and think the major factor in elevating the sea surface is the low pressure associated with the eye of the hurricane. In reality, it is the *wind shear* that raises the sea surface and the storm surge is really a dome of water on which high waves are superposed. The doming occurs as the hurricane winds drive water across the continental shelf towards land.

Two types of storm surge are distinguished here. A common misconception is that surge comes only from the ocean. In reality it first moves landward from the ocean (flood surge) and then seaward from both the rivers and bays behind the coast (ebb surge). The flood surge occurs later as the hurricane moves onshore and drives nearshore waters inland. The ebb surge occurs as the hurricane moves across the coast, permitting the entrapped surge waters and rivers engorged from rainfall to move seaward. Ebb surge is significantly less intense than flood surge, but is capable of proportionately greater destruction because it affects structures already weakened by waves, flood surge, and windborne debris.

Measuring and predicting surge levels

Techniques of measuring storm surge levels in the field have been described by Coch and Wolff (1991) from investigations in Hurricane Hugo. Three criteria are used: (1) abrasion marks made on structures and trees by floating debris; (2) heights of debris trapped or abandoned as flood waters receded; (3) stain lines from muddy waters and finely divided organic materials on building walls. It is important to exclude marks made by waves (higher than the surge level). In this regard, debris and stain lines in protected areas and enclosed rooms are the best indicators of maximum surge levels (Nelson, 1991).

The SLOSH (Sea, Lake, and Overland Surge from Hurricanes) model of the National Weather Service now provides an accurate prediction of expected surge levels along major coastal segments (Jarvinen and Lawrence, 1985). Mathematical analysis of a number of factors generates contours showing the expected height of storm surge for a given a set of conditions on

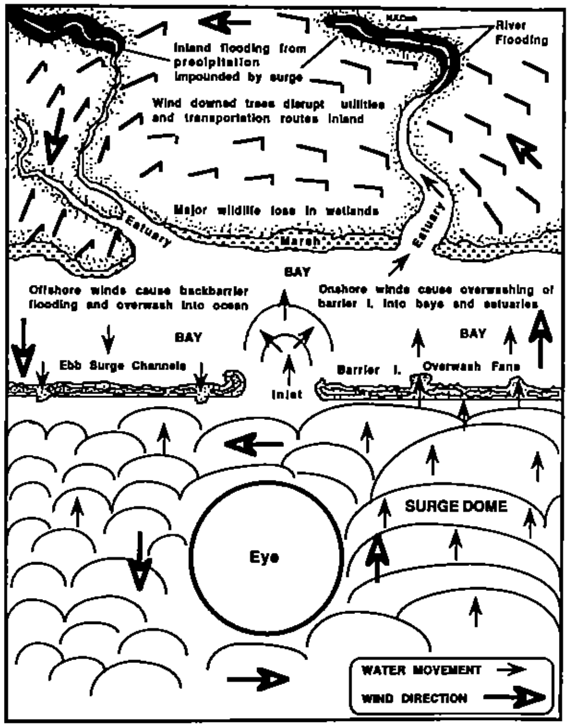

Fig. 8. Generalized map showing the variety of damage patterns associated with a coast-normal hurricane track across a barrier island-low lying coastal plain shoreline segment.

a specific shoreline segment. The pre-hurricane SLOSH analysis done for the South Carolina coast proved amazingly accurate in predicting actual surge levels in Hurricane Hugo (Coch and Wolff, 1991). One of the SLOSH maps drawn by the National Hurricane Center for the apex of the New York Bight is shown in Fig. 9. The map contours give the predicted storm surge for a Category 3 hurricane moving northwest across northern New Jersey at a forward speed of 65 km/h (40 mile/h). The reasons for the high surge values and their significance are discussed in a subsequent section of this paper.

Flood surge

The major factors determining the height of the flood surge are: (1) wind speed, (2) central pressure, (3) slope and width of the continental shelf, (4) tidal stage, (5) shoreline configuration, and (6) anthropogenic changes along the coast. All these factors aid in raising the water surface into a dome upon which wind shear will develop high waves.

The wind speed, rather than the low pressure in the eye, is the most important factor in generating flood surge. The sea surface is drawn up in the low pressure within the eye but this accounts for only a small portion

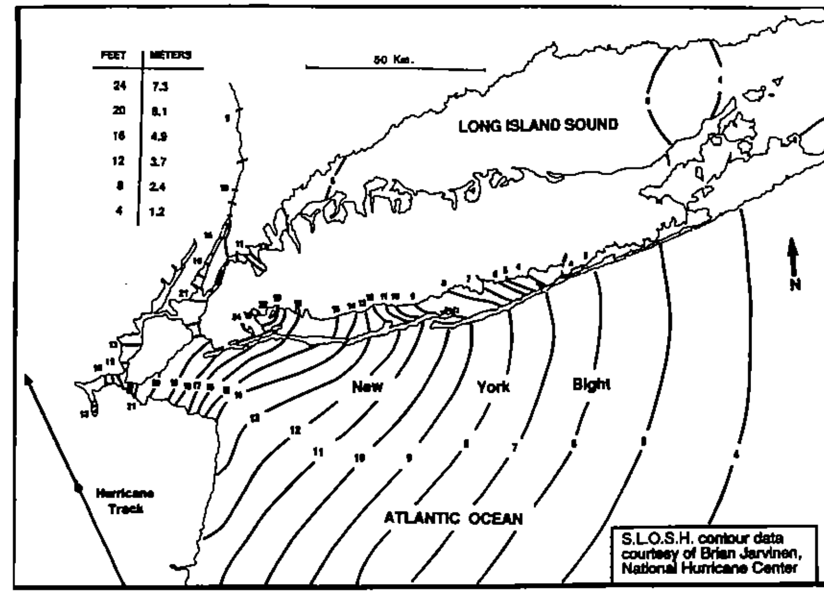

Fig. 9. SLOSH map for the apex of the New York Bight showing the predicted storm surge levels (in feet) resulting from passage of a category 3 hurricane moving NW across northern New Jersey at a forward speed of 65 km/h (40 mile/h). SLOSH contours courtesy of Brian Jarvinen, National Hurricane Center.

of the surge level because the rise is only about 0.3 m (1 ft) for an atmospheric pressure drop of 33.9 mbar (1 inch of mercury) according to Pore and Barrientos (1976). In all recent hurricanes the maximum surge has not been under the eye (where pressure is lowest) but to the right of the eye at the radius of maximum winds, where winds are greatest (Penland et al., 1989; Coch and Wolff, 1991; Coch, 1994).

The slope and width of the continental shelf exert an effect on both surge and wave height. In general, the gentler the slope the greater the surge, but the lower the waves. Conversely, the steeper the offshore slope, the lower the surge, but the higher the waves.

The steep offshore slope south of the island of Kauai produced a relatively low surge during Hurricane Iniki in 1992. The storm was a Category 4 hurricane (Table 1) but surge levels were only about 1.5–2 m (4.5–6 ft) as Iniki made landfall on the south coast of Kauai (Central Pacific Hurricane Center, 1992). However, massive 6.1–10.6 m (20–35 ft) waves pounded the many resort complexes along the coast causing extensive damage (Fig. 10). Debris lines marked surf inundation to an altitude of 6.7 m (22 ft) inland. These high values were very close to the U.S. Army Corps of Engineers "worst case scenario" for a storm in Hawaii (Central Pacific Hurricane Center, 1992).

The configuration of the coast is also important and surge height increases in concave seaward (bay) coastal sections. In Hurricane Hugo, gentle shelf slope, location at the radius of maximum winds, and a concave seaward coastal segment, combined to raise surge levels of 6 m (20 ft) at Bulls Bay, about 22 km (14 miles) northeast of Charleston (Coch and Wolff, 1991; Fig. 10).

Tidal stage at landfall can also significantly increase the height of storm surge. Surge levels can increase 1-

Fig. 10. Hurricane Iniki (1992) damage to homes along the Poipu coast of southern Kauai, Hawaii. Photograph taken one year after the storm. Massive waves destroyed the second story of this home. The surge and waves broke the stone wall, deeply eroded the lawn and deposited basalt boulders inland. Photograph by Nicholas K. Coch.

3 m (3–9 ft) at high tide depending on tidal range along a coastal segment. The path of Hurricane Gloria (1985) across highly urbanized western Long Island (Fig. 2) provides an example. Millions of people in the region were warned before landfall that this Category 3 storm could cause major damage. However, it slowed down to 48 km/h (30 mile/h) as it moved northward and it made landfall on the south shore of Long Island at low tide, resulting in a surge of only 1.5 m (5 ft). Thus, after a big media build-up the surge damage was minimal (although winds wreaked extensive tree damage and other havoc inland). Consequently, inhabitants of the northeast United States resumed their complacency, believing major hurricanes do not affect northern coastal areas. In reality, they were just lucky. If Gloria had hit at high tide, with all the other factors the same, the surge would have been 3 m (10 ft) above sea level at the Battery in New York City. Each borough of New York City would have experienced tidal flooding on an average distance of 61 m (200 ft) inland from the shore. The expected damage and dislocation of regional transport in the New York Metropolitan area is presented by Gigi and Wert (1986, pp. 3–6).

The worst case scenario for storm surge is approximated by the 1938 New England Hurricane (Fig. 2). This high Category 3 storm (B. Jarvinen, pers. commun., 1993) was moving forward at greater than 96 km/h (60 mile/h) and hit the south shore of Long Island at just about high tide. Surge levels as recorded by high water marks (Pore and Barrientos, 1976) reached from 2.1 m (7 ft) to 4.8 m (15.6 ft) along the south shore of Long Island.

The geographic orientation and shape of a coastal segment can also exert a major effect on amplifying storm surge. Coastal segments along the Atlantic Coast of the United States that amplify storm surge are right angle segments and funnel-shaped estuaries that open to the east. Both of these types of shoreline segments exist close together in the apex of the New York Bight and in Long Island Sound to the north (Fig. 11). When a hurricane enters the New York Bight, the counter-clockwise (easterly) flow of winds around the front of the storm center drive the waters into the right angle made by the New York–New Jersey juncture, increasing surge levels westward. This surge amplification was the cause of a great deal of damage in the shore communities of western New York and northern New Jersey in the "nor'easter" storms of December 1992 (Coch, 1994).

The worst case scenario for surge damage in the New York Bight region (B. Jarvinen, pers. commun., 1993) is for a hurricane passing over northern New Jersey. The SLOSH prediction for that scenario would have water levels rising to 6.4 m (21 ft) at the entrance to

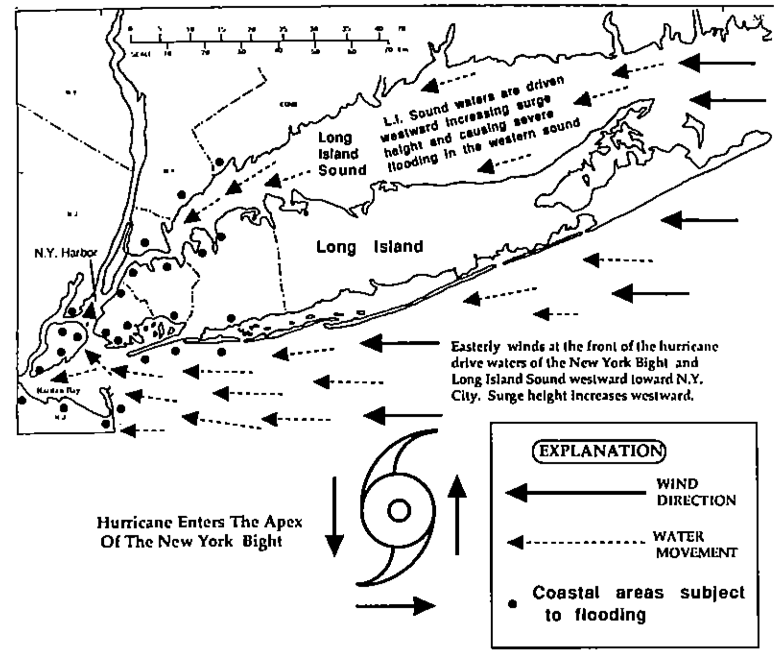

Fig. 11. Storm surge amplification in the apex of the New York Bight and in Long Island Sound. The easterly winds at the front of a hurrica entering this region drive both the waters of the New York Bight and Long Island Sound westward causing severe flooding during landfall an passage across Long Island.

New York Harbor at the Narrows and 7.3 m (24 ft) in Jamaica Bay at the western end of Long Island (Fig. 9).

The same hurricane winds that drives New York Bight Apex waters westward also drive the waters of Long Island Sound westward. Long Island Sound is an east–west oriented funnel-shaped estuary opening to the east. This is the direction from which hurricane winds come as the storm moves into New England (Fig. 11). Long Island Sound varies in width from 27 km near its eastern end to less than 3 km at its western end in New York City. The easterly winds at the front of the hurricane drive the waters of the Sound westward, through a decreasing cross section, towards New York City as the hurricane approaches the south shore of Long Island. However, the progressive wave take about three hours to move westward across the Soun so that maximum surge levels are attained in the wes ern end of the Sound when the Hurricane is in centr New England (B. Jarvinen, pers. commun., 1993).

Some indication of the degree to which surge amplified in a funnel shaped estuary like Long Islar Sound is available from measurements made in tl 1938 Hurricane (Pore and Barrientos, 1976). Surge the eastern part of the sound was about 2.3 m (7.5 f increasing steadily to a maximum of 3.9 m (12.7 ft) the entrance to the East River in New York City (Fi 12).

This hurricane had made landfall on the south sho of Long Island at 3:30 p.m. and moved inland at

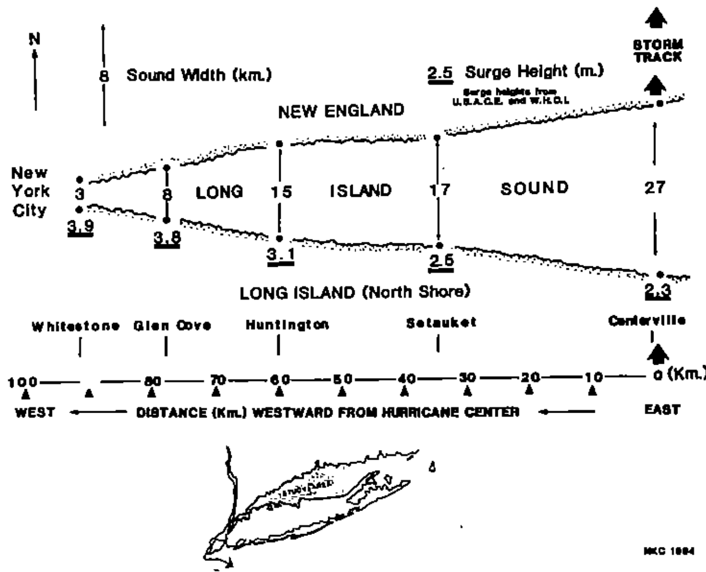

Fig. 12. Map of surge levels in Long Island Sound in the 1938 New England Hurricane. Surge heights increased steadily westward as the estuary narrowed. The maximum surge level at the western end of the sound (New York City) was reached three hours after the hurricane made landfall on the south shore of Long Island. Based on data in Pore and Barrientos (1976). The shoreline of Long Island Sound has been generalized, but widths and distances are accurate.

velocity of 80–96 km/h (50–60 mile/h). However, the maximum storm surge in western Long Island and the East River in New York City was reached *three hours later*, about 7:30 p.m. Rising surge waters flooded lowlying areas of the Borough of Queens in New York City and inundated hospitals and power plants on islands in the East River. The inundation of the power plant near Hell Gate in the East River plunged parts of the Boroughs of the Bronx, and Manhattan into darkness, as well as bringing part of New York City's subway system to a halt. At this time (7:30 p.m.) the hurricane center was in northern Vermont (Bricker, 1988).

Ebb surge

Ebb surge is the seaward return of water impounded on land as the hurricane moves inland. The height of the ebb surge is a function of the flood surge, the amount of precipitation preceding and during the hurricane and the local obstructions that block flow back into the ocean. Ebb surge is lower than flood surge, but can still cause significant damage because it affects structures that were partially destroyed by flood surge, wave action, and wind borne debris (Fig. 13).

A number of factors increase the possibility of ebb surge damage at a given location. These factors include; (1) failure or absence of shore protection structures (rip-rap aprons, bulkheads); (2) streets that run perpendicular to the shoreline; (3) areas of open land with little vegetation and; (4) presence of beach access paths, dune walkovers, and locations on narrow parts of barrier islands seaward of bays (Lennon, 1991).

The damage done by ebb surge is more elusive than the visible "dams" of debris washed inland by flood surge (Fig. 13). Side-scan sonar studies of the South Carolina nearshore zone by Gayes (1991b) after Hurricane Hugo have provided new information on the erosional and depositional dynamics of ebb surge. The study detected 30–50 m (98–164 ft) wide channels perpendicular to the shoreline that cut through shore oblique bar systems parallel to the shore. Side-scan sonar sweeps and diver observations documented a wide variety of debris scattered over the nearshore area (Gayes, 1991b; Fig. 13) up to 100 m (328 ft) offshore in water depths of 2–4 m (7–13 ft). Specific types of debris recognized during the study included portions of fishing piers, seawalls, and mobile homes (P. Gayes, pers. commun., 1991a). Development along the shore of the study area correlated well with locations of many scour channels. Massive multi-storied structures not raised on pilings had clearly obstructed, diverted and channeled the storm surge and there was frequently a noticeable absence of a well-developed nearshore bar and the presence of steeper beachface slope in those areas.

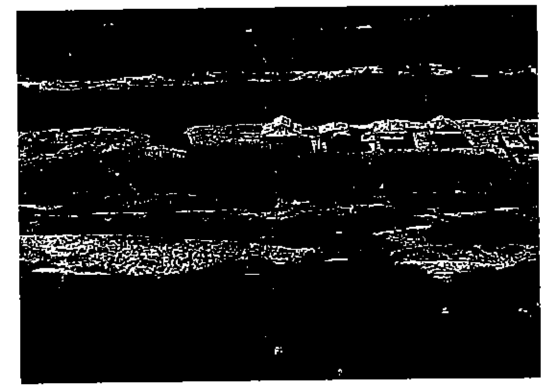

Fig. 13. Ebb surge cut channel at Pawleys Island, South Carolina formed in Hurricane Hugo (1989). Two homes were lost and bulkheading was destroyed by the ebb surge. Note the flood-surge deposited debris at the edges of the trees at the top of the photo. Photograph by Nicholas K. Coch.

3.2. Wind

Wind and storm surge cause the major damage along the coast. Inland, wind is the dominant cause of damage. In a hurricane with a coast-parallel track (Fig. 6), wind damage drops off rapidly inland. However, in a hurricane with a coast normal track (Fig. 6), winds can cut a wide swath of devastation far inland.

Scales of wind damage

A common conception about hurricane wind damage is that the storm cuts a continuous swath across the land. Remote sensing, and post-hurricane ground and aerial damage analysis suggest that the damage is far more uneven. It is clearly more intense near the eyewall area (Fig. 3), but in outlying areas the intensity of damage may simply be a matter of chance.

Three scales of wind damage are used in this paper to describe wind damage effects (Fig. 14). The sum total of all damage over the diameter of the storm makes up the *megascale* pattern (Fig. 14). The second scale of damage is the *mesoscale* pattern and involves differential convective activity within the rainbands spiraling around the eye and the areas between the rainbands (Fig. 3). The higher Doppler Radar reflectivities (Db values in Fig. 14) associated with the rainbands reflect the greater degree of radar impulse return from the raindrops in the bands. Simply put, under an area of higher radar reflectivity such as in the rainbands in Fig. 14, there will be more severe damage than to either side. An actual example will be described later in this paper.

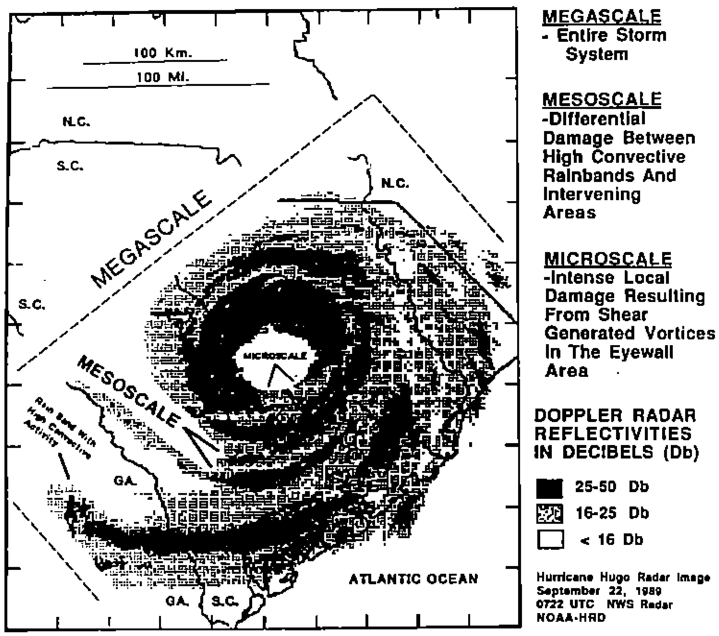

Fig. 14. Three scales of wind damage in a hurricane. The megascale pattern is the sum total of all damage across the diameter of the storm. The mesoscale pattern describes differential damage between highly convective areas on the rainbands and the areas in between. Microscale patterns of damage are narrow, local paths of extreme destruction caused by spin-up vortices described by F. Fujita in Hurricane Andrew.

The smallest scale of damage is the *microscale* pattern that is most common in the eyewall area (Fig. 14). Microscale damage was described by Prof. F. Fujita, of the University of Chicago, from aerial photograph analysis and field surveys after Hurricane Andrew. Aerial photographs of Andrew's impact zone in South Dade County, Florida showed scattered, narrow, short and curving paths of extreme damage within an overall severely devastated area. Fujita (1993) believes that these damage patterns result from *spin up vortices* generated in the eyewall. According to Fujita (1993), slowly rotating vortices 60–152 m (200–500 ft) in diameter form as a result of slight variations in wind speed along the eyewall. If these vortices migrate inward, into the calmer area in the eye, they dissipate. However, if the vortex migrates outward, under an area of high convective activity, the results are quite different. The convection stretches the vortex upward, reducing its diameter and increasing its speed in the process. Vortex velocity now may reach 129 km/h (80 mile/h). However, the small spin up vortex is imbedded in the faster hurricane winds moving at 193 km/h (120 mile/h), leading to *effective* winds of 322 km/h (200 mile/h). This type of microscale activity caused extreme damage in the Naranja Lakes and Pine Woods Villa developments in South Dade County, Florida in Hurricane Andrew (Fujita, 1993).

Sustained versus peak velocities

Hurricane wind velocities are generally reported as *sustained winds*, persisting at that level for several minutes. However, *gust velocities* persisting for short

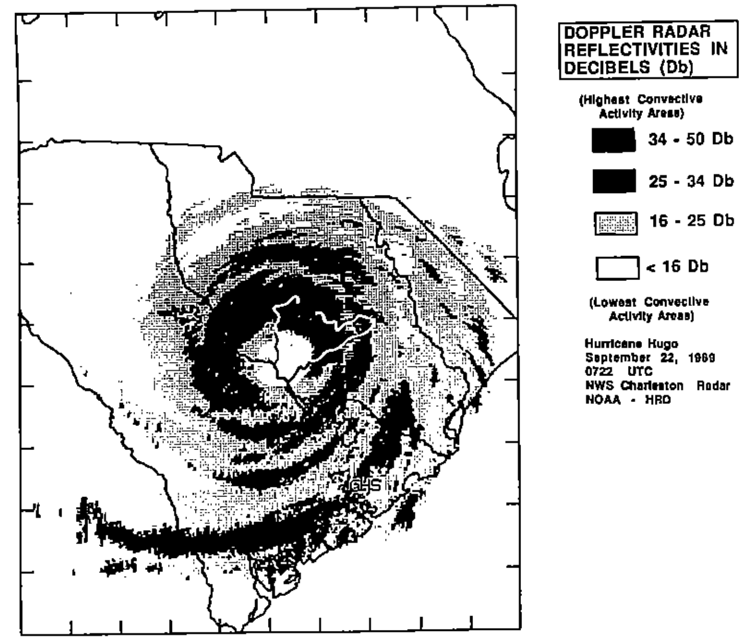

Fig. 15. Doppler Radar image of Hurricane Hugo when the eye and eyewall area was located over inland Sumter County (outlined area). Areas of extreme convective activity (34–50 Db areas on the diagram) resulted in peak gust winds far greater than the mean winds of the weakening hurricane.

duration are important because gusts can exceed sustained winds by up to 100% in highly convective situations. Gust speeds are estimated by applying a gust factor to the mean wind of a given averaging period. Krayer and Marshall (1991) derived a gust factor of 1.5 based on a study of major hurricanes. As a hurricane moves inland, its sustained winds drop as a result of frictional effects and a filling-in (weakening) of the storm. Studies done after Hurricane Hugo (Powell et al., 1991) have shown that isolated convective centers inland (Fig. 3) can generate wind gusts as strong as the hurricane's earlier sustained winds at landfall. This results in unexpectedly severe damage 60 km (100 miles) or more inland from the coast.

The effect of peak gust winds inland was well demonstrated during Hurricane Hugo in Sumter County, South Carolina (Fig. 15). As Hurricane Hugo passed over Sumter County, its winds had decreased from Category 4 at the coast to just above Category 1 (Table 1). However, the right eyewall of the storm containing areas of high convective activity, passed over a good part of the county and was to create mesoscale-pattern damage (Fig. 14). The 10-minute gust factor approached a value of 2.0 because of the presence of extremely convective rain band features (Fig. 15) during eyewall passage (Powell et al., 1991). Thus, while the mean wind speed was about 121 km/h (75 mile/h), or a Category 1, a good part of the county was being battered by *Category* 4 level winds of up to 225 km/h (140 mile/h) and destruction was severe in a county far inland from the ocean (Fig. 15). The inhabitants of the county had expected to shelter refugees from coastal destruction but instead required massive help themselves. Damage in Sumter County exceeded 790 million dollars and 75% *of all injuries* during Hurricane Hugo occurred in Sumter County (V. Jones, pers. commun., 1993).

Wind damage factors

Wind damages structures and vegetation by its force, pressure differential effects and by creating and transporting debris that destroys other structures. The force exerted by the wind varies with the square of the velocity. Thus a 3× increase in wind speed from gale force winds of 55 km/h (34 mile/h) to Category 2 hurricane winds of 164 km/h (102 mile/h) increases the wind force 9 *times* (3^2). The inverse relationship between air flow and fluid pressure creates areas of differential pressure around a structure. Where the wind flows faster, the pressure is lower, and vice versa. The differential pressure fields around a structure may cause it to fail (Fig. 16). The side of a structure facing the wind is subject to compressive stresses that tend to push the wall and windows in. The faster moving air flowing over the roof and around the sides of the structure generate areas of low pressure that act as suction forces,

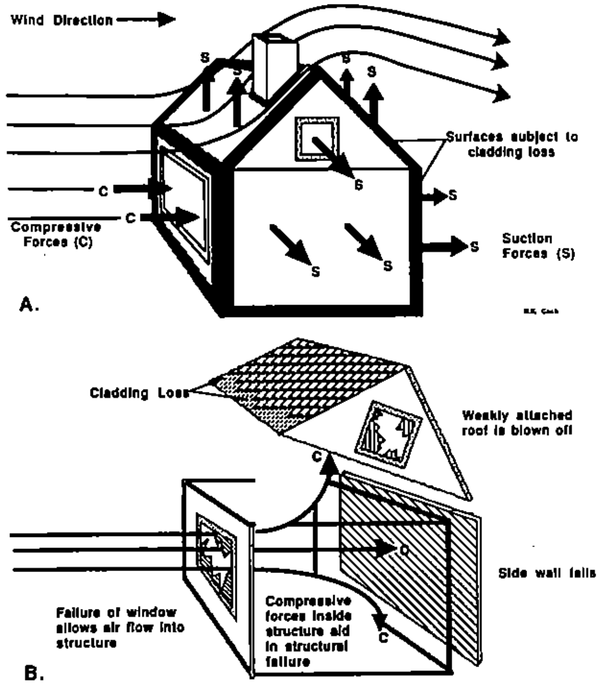

Fig. 16. (A) Wind forces acting on a structure in a hurricane. The side facing the wind is subject to compressive forces that tend to push it in. The faster moving air flowing around the sides and roof create a low pressure zone that results in suction forces tending to pull the structural walls outward. As long as the structure remains intact it may resist these forces. (B) the integrity of the structure has been destroyed by debris that broke a window, the free flowing air inside the structure now pushes outward on the walls and roof and the structure is destroyed. Diagram by the author suggested by descriptions in Sparks (1991).

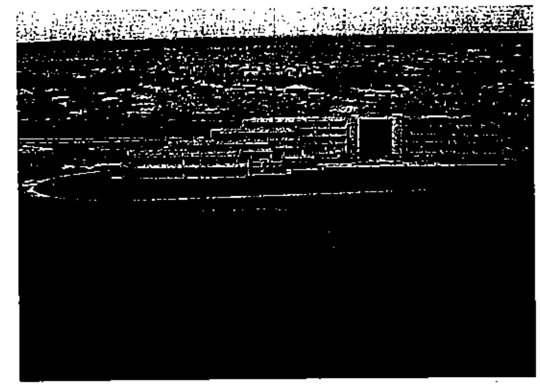

Fig. 17. Hurricane Andrew surge and wind destruction at the national headquarters of the Burger King Corporation on Biscayne BayW, Florida. This location, near the radius of maximum winds of Hurricane Andrew, experienced the highest surge and winds. The lower story was gutted by surge while the upper ones were destroyed by winds. Aerial photograph by Nicholas K. Coch.

tending to pull the walls and roof outward (Fig. 16A). The structure can therefore fail if: (1) structural walls are weak; (2) the roof, walls, and foundation are not held together by combinations of reinforcing plates and straps; or (3) if wind can gain access to the inside of a structure through structural failure or airborne debris damage to windows, home doors, or garage doors. If wind enters the structure, it exerts a compressive force on the interior walls and roof that acts with the suction forces outside to tear the structure apart (Fig. 16B). In Hurricane Andrew, rolling garage doors were shifted off their tracks by sustained winds and gusts, allowing

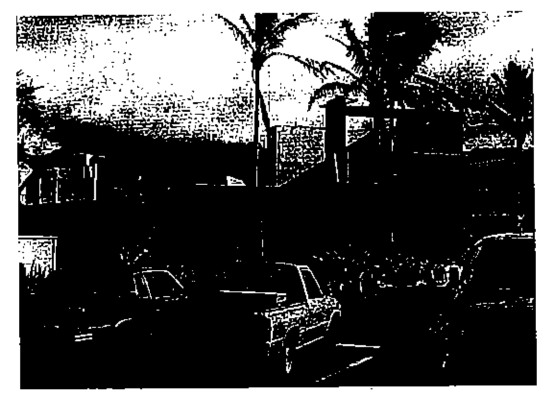

Fig. 18. Homes gutted and trees damaged by the high winds of Hurricane Iniki (1992) at Princeville, Kauai. Photograph taken one year after the storm, these homes were on a ridge fully exposed to winds that were channeled through the mountains in the distance. The channeling increased the wind speed, resulting in great damage on the lee side of the island. Photograph by Nicholas K. Coch.

wind to gain access to many homes (FEMA, 1993a).

Exposure is also an important factor in wind damage. Homes in South Dade County, Florida that had open spaces (parks, lakes, vacant sites, etc.) upwind of them sustained greater damage in Hurricane Andrew. (R. Sheets, pers. commun., 1993). Exposure along a coast is also a factor. Homes nearest the coast are affected by unimpeded flow that decreases rapidly inland as a result of frictional drag over topographic features, structures, and vegetation. An extreme case of wind velocity decrease inland was reported by SethuRaman (1979) before Hurricane Belle (1976) made landfall on the south shore of Long Island. Anemometer readings 10 km inland were 50% of those at the coast, and readings 20 km inland were 25% of the coastal values (SethuRaman, 1979)

The effects of wind increase away from the ground surface where friction with the topography, structures and vegetation slow down air flow. The problem is especially serious along urbanized coasts where high rise buildings are subject to increasing wind velocities on their upper floors while the lowest floors are being destroyed by storm surge (Fig. 17).

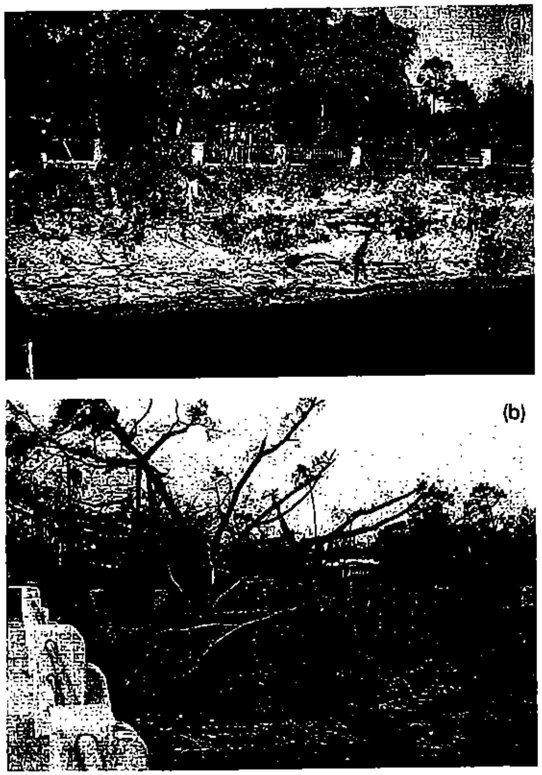

Fig. 19. Changes in the landscape accompanying Hurricane Andrew (1992) at the Coral Gables Canal, Dade County, Florida. (a) Before Andrew (1987) the cross bedded oolite outcrop is well exposed and lush vegetation covers the area in the distance. (b) After Andrew (1992) the trees are broken and defoliated and the house in the distance is fully exposed. Photographs by Nicholas K. Coch.

Hurricane Iniki (1992) made landfall on the island of Kauai, Hawaii and provided a good view of the effects of a hurricane on a mountainous island. Wind speeds increased as the flow was channeled through mountainous passes to cause unexpected devastation on the *lee side* of the island (FEMA, 1993b). Destruction of homes and vegetation on ridge crests was especially severe (Fig. 18). Debris mobilized by hurricane winds caused significant damage. Pieces of structures, such as the corrugated roofs widely used on Kauai, served as projectiles that damaged other structures. Loss of glazing (windows), allowed storm winds to enter the structure (Fig. 16B) and assist in its disintegration (FEMA, 1993b).

4. Geologic changes in hurricanes

Dramatic changes in the landscape occur after a major hurricane (Fig. 19). Structural damage may be restored in weeks or months, but vegetation may take far longer to recover. The vegetation loss may significantly increase the danger of forest fires as well as increasing soil erosion and gullying. However, the most dramatic geologic changes occur near the coast and involve beach and dune erosion, barrier island breaching and nearshore channeling by ebb surge.

4.1. Beach erosion

Elevated storm surge and high waves cause severe beach and dune erosion. Stauble et al. (1991) noted that Hurricane Hugo (1989) reduced most of the dunes over a 160 km (110 miles) stretch on the right side of the storm to a flat planar surface while others were severely eroded. Where winds and surge were highest in Hurricane Hugo, barrier sands were eroded away to expose the underlying peat (Fig. 20). The sand was transported landward as overwash fans built into water bodies behind the shoreline.

Nelson (1991) utilized before and after topographic surveys to describe beach and dune alteration (Fig. 21) from Hurricane Hugo (1989) in South Carolina. In most cases, there was significant recession of the beach face. Some examples of beach face recession are: North Myrtle Beach, 19 m (62 ft); Myrtle Beach, 8.5 m (28 ft); Surfside Beach, 8.5 m (28 ft); and Garden City Beach, 12.8 m (42 ft). The profile at Surfside Beach (Fig. 21) showed a flattening and recession of the beach face, and the development of an overwash apron and nearshore bar as a result of the storm.

Fig. 20. Flood surge erosion and deposition on the barrier island south of Bulls Bay, South Carolina. This area was at the radius of maximum winds in Hurricane Hugo (1989). Sand was stripped from the beach and deposited as overwash fans (light areas) into the bay behind the barrier island. An underlying peat deposit (dark layer) is now exposed along the ocean shoreline (right side of photo). Aerial Photograph by Nicholas K. Coch.

4.2. Dune erosion

Dune erosion in hurricanes depends on dune height, width, and vegetation. The best documentation of the extent of dune erosion in hurricanes comes from studies done by several groups after Hurricane Hugo (1989) in South Carolina. This Category 4 event leveled dunes, reducing them to planar surfaces or severely eroding

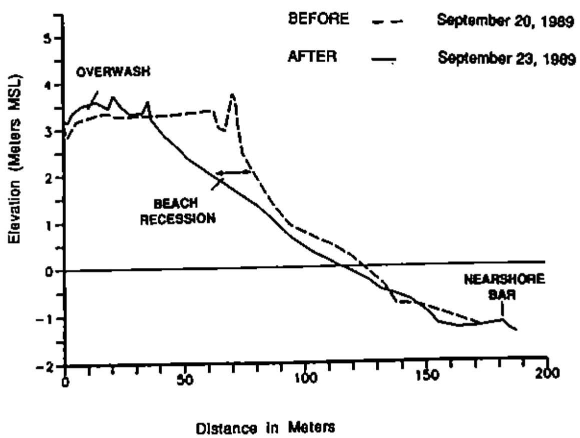

Fig. 21. Before and after topographic profile at Surfside Beach, South Carolina showing erosion and deposition from Hurricane Hugo (1989). The beach face was flattened and receded, and an overwash apron and a nearshore bar were formed. Modified from Nelson (1991).

them over a 160 km (110 miles) stretch from north of the eye at Myrtle Beach to south of the eye at Folly Beach (Stauble et al., 1991). Thieler and Young (1991) found that dunes survived when high enough to prevent their being overwashed and wide enough to prevent being completely eroded. A good example of this were the dunes at Litchfield, South Carolina that were scarped and cut back but not destroyed. Prior to the storm, the dunes reached up to 7 m (23 ft) and dune width was 15 m (49 ft) according to Stauble et al. (1991). The other situation where dunes survived was when they were low but well vegetated so that they could be rapidly submerged without significant erosion such as occurred at Sullivans Island and the Isle of Palms near the eye of Hugo (Thieler and Young, 1991). The only problem with this type of "dune survival" is that it provides little protection for structures behind the dunes.

4.3. Vegetation loss and soil erosion

Loss of vegetation provides a striking change in the landscape after a hurricane (Fig. 19) and has a great impact on birds and animals (Coch, in prep.). In this paper only the geological aspects of vegetation loss are considered.

Hurricanes Hugo, Andrew, and Iniki showed the wide range of damage that results from the uprooting, bending and breaking of trees Falling trees cause structural damage and bring down utility lines. They also block roads needed for access by emergency vehicles. The roots of overturned trees break underground water and utility lines. This type of tree damage caused major disruption when Hurricane Hugo (Fig. 15) crossed over Sumter County, South Carolina (V. Jones, pers. commun., 1993).

The patterns of tree fall are not random but are relatively uniform *at any one place*. There is usually a significant difference in tree fall orientation on either side of a hurricane (Fig. 8). This has been documented by detailed plots based on analysis of aerial photographs (Penland et al., 1989, fig. 6). In general, the pattern of tree fall orientation (Fig. 8) in landfall areas is controlled by the wind directions at the front of the hurricane (Fig. 4). However, the tree fall orientation in inland areas may be much more complex and variable.

The number of trees downed and the type of failure (bending, breaking, loss of upper canopy only, etc.) is a function of both tree type and location with respect to the eyewall. Hook et al. (1991) compared tree loss

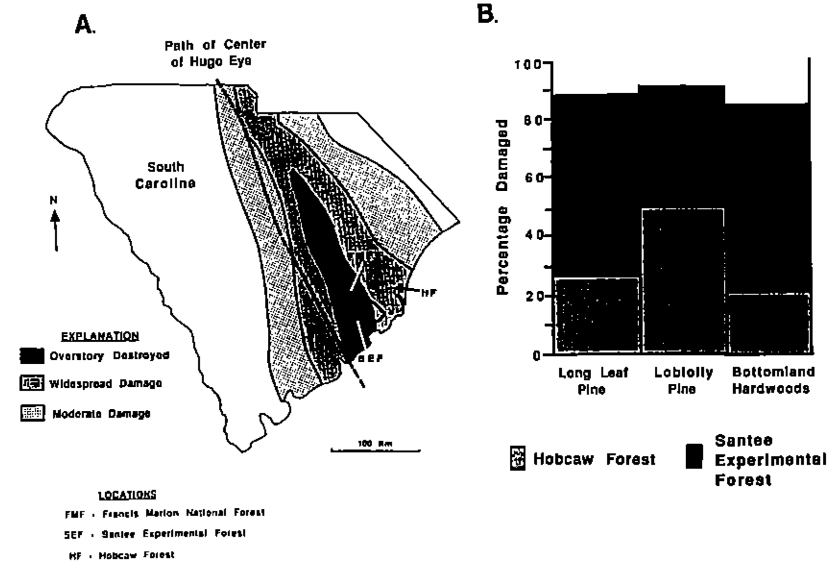

Fig. 22. Comparison of tree damage in two South Carolina Forests during Hurricane Hugo (1989). Damage to all species studied was severe in the Santee Experimental Forest close to the eye of the storm. Damage was far less, and species dependent, in the Hobcaw Forest on the outer part of the storm. (Modified from Hook et al., 1991).

Fig. 23. Photograph of extensive tree breakage and deforestation on Kauai, one year after Hurricane Iniki (1992) struck the area. Massive tree destruction occurred as a result of wind acceleration, near the ridge crest in Waimea State Park, Kauai. Photograph by Nicholas K. Coch.

Fig. 24. Gullying and soil erosion resulting from Hurricane Iniki (1992) on Kauai Hawaii. Photograph taken one year after hurricane. The high rainfall and steep slopes in Waimea State Park on Kauai accelerated soil loss and gullying when vegetation was destroyed at higher altitudes. Photograph by Nicholas K. Coch.

in two South Carolina forests during Hurricane Hugo. The Santee Experimental Forest was in the Francis Marion National Forest within the right eyewall of Hurricane Hugo (Fig. 22) 41–58 km north of the eye center. Winds there during the storm were 43–66 km/s (27–41 mi/h). The Hobcaw Forest was 83–108 km north of the eye center and was subjected to considerably less wind force than the Santee Forest. In the Santee Forest there was little difference between the wind resistance of different species. The percent damaged were as follows (Fig. 22); long leaf pine (89%); loblolly pine (91%); and bottom land hardwoods (86%). In the Hobcaw Forest the damage was considerably less and was species dependent. Damage percentages were as follows: long leaf pine (27%); loblolly pine (52%); and bottom land hardwoods (20%).

Loss of vegetation can have significant geological consequences, especially in mountainous areas with high rainfall. Hurricane Iniki (1992) a Category 4 storm, caused widespread tree damage on the island of Kauai, Hawaii (Fig. 23). Uprooted trees exposed the soil to erosion. The high rainfall plus the steep slopes substantially increased the rate of soil erosion and gullying (Fig. 24).

Re-vegetation after a hurricane in tropical and subtropical areas is much faster than in temperate climates. Data from the 1938 New England Hurricane shows that a major hurricane hitting the mountainous areas of the northeastern United States will cause significant deforestation (Federal Writers Project, 1938). Re-growth will take years and high rates of soil erosion as well as the threat of forest fires will persist during the recovery period.

5. Summary and conclusions

Hurricanes cause a wide variety of damage including flood and ebb surge, wind destruction and inland flooding. Hurricanes with coast-parallel tracks cause significant damage along a long stretch of coast, but the effects drop off rapidly inland. Hurricanes with coast-normal tracks affect a shorter section of shoreline but far more severely. In addition, they cut a wide swath of destruction hundreds of kilometers inland. The destructive power of hurricane winds is not only a function of the vortex velocity but also the forward velocity of the storm center. On the right side of the hurricane, the two wind speeds are vectorially added, greatly increasing the effective wind speed in that sector. The increase in hurricane center speed as the storm passes north of Cape Hatteras and becomes affected by stronger westerly winds, gives northeast United States landfalling hurricanes far more destructive power than storms of similar Saffir–Simpson categories that impact southern coasts.

Storm surge is the rise in the ocean surface resulting from hurricane winds driving shelf waters into shallower areas nearshore as well as the rise in the surface resulting from the low pressure in the eye of the storm. Storm surge is more accurately pictured as a broad dome of water on which high waves usually develop. Maximum surge levels occur on the right side of the storm at the radius of maximum winds and levels rise higher along coasts that have gently sloping continental shelves and embayed sections. Potential surge is highest along segments that make right angles opening eastward, such as the New York Bight and along funnel-shaped estuaries opening east, such as Long Island Sound. Surge amplification has caused especially serious damage along these two highly urbanized coastal segments both in the great "nor'easter" storms of the 1990's (Coch, 1994) and in every hurricane that has made a landfall along the coast of Long Island, Rhode Island or southern Massachusetts (Pore and Barrientos, 1976). Ebb surge occurs as impounded flood surge waters and previous rainfall move seaward as the hurricane passes inland. Although ebb surge is much lower in height than flood surge, ebb surge can cause considerable erosion because it affects structures that have already been weakened by winds and flood surge as well as debris carried by both agents. Ebb surge overwashes barrier islands from the bayward side, disperses debris across the nearshore zone to create navigational hazards, and cuts inlets across the barrier islands (Fig. 13)

Hurricane winds are the major destructive force inland. Wind is especially destructive along exposed coasts and the effects drop off inland as frictional effects and hurricane filling decrease wind speed. While the overall power of a hurricane decreases inland, local convective centers on the rainbands can cause severe local damage. Wind damage occurs on storm-wide levels (megascale), associated with local high convective centers on the rainbands (mesoscale) and in very local, but extremely intense, "spin-up vortices" (microscale features) associated with the right eyewall of the storm.

Hurricanes result in considerable geologic change along the coast and inland. Beaches are stripped of sand that is deposited as overwash fans into bays. Dunes that are not high enough, or well vegetated are eroded and breached in many cases. Low, but well vegetated dunes may be overstepped with little erosion, although this provides little protection for structures landward of the dunes. The great tree destruction inland disrupts transportation and communication lines as well as buried utilities, and creates a severe fire hazard. Hurricane-induced vegetation loss in humid mountainous terrain can significantly increase soil erosion until cover is restored.

Atlantic-landfalling hurricanes seem to be more frequent during multi-decadal wet cycles in west Africa, and far less frequent in dry cycles. No wet or dry cycle has lasted longer than 26 years, and we are now in the 24th year of a dry cycle. Unfortunately, this period of quiescence has coincided with great urbanization along the Atlantic Coast and the development of public apathy toward the hurricane threat. If past climatic patterns continue, we will soon be entering a cycle of far more frequent Atlantic Coast landfalling hurricanes. These future storms will affect a heavily developed and populated coast where inhabitants have made little preparation to minimize destruction and loss of life. The result could be devastation on a scale last experienced in the northeast during the New England Hurricane of 1938. Unfortunately, it has been 56 years since that regional catastrophe, and its many lessons have been largely ignored or forgotten.

Acknowledgments

A number of colleagues and government officials were of great help in the author's four post-hurricane field studies. My special thanks to Mel Nishihara, hurricane program manager for the State of Hawaii, who set up meetings with emergency management officials on Oahu and Kauai and briefed the author on Hurricane Iniki damage. Glenn Trapp, National Weather Service, Honolulu, provided satellite images of Iniki and a preliminary science report on the storm that was of great help in field studies. Tom Batey, Administrator, County of Kauai, suggested damage study sites that facilitated field work on Kauai and he graciously discussed the results and interpretations of the observations afterwards with the author.

Sam Houston, Hurricane Research Division NOAA, discussed his preliminary findings on Hurricane

Andrew and suggested field study sites to the author three days after that hurricane devastated south Dade County, Florida. Billy Wagner and Andy Eads, Monroe County Emergency Management, gave valuable insights into damage patterns and recovery problems in the Homestead-Florida City areas.

Don Thompson, Long Island Weather Observers, provided information on Hurricane Bob meteorological effects and damage types in easternmost Long Island and accompanied the author in the field. Ana Butler conducted Hurricane Bob damage studies on Cape Cod, Mass. and graciously provided access to the data and photographs for this paper.

Hurricane Hugo field studies (Coch and Wolff, 1991) were aided by the information and logistical support provided by Paul Gayes and Doug Nelson of the Center for Marine and Wetlands Studies, Coastal Carolina College. In late 1993, Gayes and Nelson also provided an update and further information on Hugo ebb surge and dune destruction, respectively. Mark Powell, Hurricane Research Division NOAA, supplied the Hugo radar images used in this paper. Victor Jones, Director of Public Safety in Sumter County, South Carolina, described the inland effects of Hurricane Hugo and the recovery problems that ensued after the passage of the storm.

The staff of the National Hurricane Center, particularly Robert Sheets, Brian Jarvinen, Miles Lawrence, Jack Bevan and John Pavone, deserve special thanks for providing information on a number of different aspects of hurricanes over the past few years. William Gray, Colorado State University, has discussed his research on hurricane frequency with me on a number of occasions. Mike Wylie and Tony Gigi, National Weather Service, New York City, gave valuable insights into the damage done by "nor'easter" storms and by hurricanes impacting the northeastern United States. Fred Wolff, Hoffstra University provided valuable additions and corrections to the manuscript.

This research was sponsored in part by PSC-BHE grants #663177, #664048 and #771762. Drafting and word processing assistance was given by Henry Mesa, Sara Woolley and Katherine Andrade. Nancy Bareis and Matt Dinzie, Photographic Unit, CIMS at Queens College, produced the photo plates for this paper. My special thanks to Katherine Andrade for her overall administrative help in the production of this paper.

References

Bricker, R.K., 1988. The Long Island Express — Tracking the Hurricane of 1938. Hodgins, Batavia, NY, 125 pp.

Carter, T.M., 1983. Probability of hurricane/tropical storm conditions: A user's guide for local decision makers, U.S. Dept. Commerce, NOAA, NWS Severe Weather Branch, 25 pp.

Central Pacific Hurricane Center, 1992. Preliminary Science Report, Hurricane Iniki, September 5–13, 1992, Honolulu, Hawaii.

Coch, N.K., 1994. The hurricane hazard in the northeastern U.S. In: C.W. Finkl (Editor), Coastal Hazards. Perception, Susceptibility and Mitigation. J. Coast. Res., Spec. Vol., 12, in press.

Coch, N.K. and Wolff, M.P., 1990. Probable effects of a storm like Hurricane Hugo on Long Island N.Y. Northeast. Environ. Sci. 9 (1/2): 1–14.

Coch, N.K. and Wolff, M.P., 1991. Effects of Hurricane Hugo storm surge in coastal South Carolina. In: C.W. Finkl and O.H. Pilkey (Editors), Impacts of Hurricane Hugo: September 10–22, 1989. J. Coast. Res. Spec. Issue, 8: 201–228.

Federal Writers Project, Works Progress Administration in the New England States, 1938. New England Hurricane — A Factual Pictorial Record. Hale Cushman and Flint Co., Boston, 220 pp.

FEMA, 1993a. Building Performance in Hurricane Andrew in Florida. FIA-22: 93.

FEMA, 1993b. Building Performance in Hurricane Iniki in Hawaii. FIA-23: 100.

Fujita, T., 1993. Origin of spin-up vortices. Am. Meteorol. Soc. address, Summarized in Earth, 2(4): 11.

Gayes, P., 1991a. Personal communication, Center for Marine and Wetland Studies, Coastal Carolina College, Conway, SC 29526, USA.

Gayes, P., 1991b. Post-hurricane Hugo nearshore side scan sonar study: Myrtle Beach to Folly Beach, South Carolina. In: C.W. Finkl and O.H. Pilkey (Editors), Impacts of Hurricane Hugo: September 10–22, 1989. J. Coast. Res. Spec. Issue, 8: 95–112.

Gigi, A.F. and Wert, D.A., 1986. Hurricane Gloria's potential storm surge. NOAA Tech. Mem. NWS ER-70, July 1986.

Gray, W.M., 1990. Strong association between West African rainfall and U.S. landfall of intense hurricanes. Science, 249: 1251–1256.

Gray, W.F. and Landsea, C.W., 1991. Predicting U.S. hurricane spawned destruction from west African rainfall. Unpubl. report, Dept. Atmospheric Sciences, Colorado State University, Fort Collins, CO, 40 pp.

Hook, D.L., Buford, M.A. and Williams, T.M., 1991. Impact of Hurricane Hugo on the South Carolina Coastal Plain Forest. In: C.W. Finkl and O.H. Pilkey (Editors), Impacts of Hurricane Hugo: September 10–22, 1989. J. Coast. Res. Spec. Issue, 8: 291–300.

Jarvinen, B.R., 1993. Personal communication, National Hurricane Center, 1320 South Dixie Highway, Coral Gables, FL 33146, USA.

Jarvinen, B.R. and Lawrence, M.B., 1985. An evaluation of the SLOSH storm- surge model. Am. Meteorol. Soc. Bull., 66(11): 1408–1411.

Jones, V.C., 1993. Personal communication, Director, Office of Public Safety, Sumter County, SC 29150, USA.

Krayer, W.R. and Marshall, R.D., 1991. Gust factors applied to hurricane winds. Preprints: Eight Int. Conf. on Wind Engineering. Assoc. for Wind Engineering, London, Ont., Canada.

Lennon, G., 1991. The nature and causes of hurricane-induced ebb scour channels on a developed shoreline. In: C.W. Finkl and O.H. Pilkey (Editors), Impacts of Hurricane Hugo: September 10–22, 1989. J. Coast. Res. Spec. Issue, 8: 237–248.

Nelson, D., 1991. Factors effecting beach morphology changes caused by Hurricane Hugo, Northern South Carolina. In: C.W. Finkl and O.H. Pilkey (Editors), Impacts of Hurricane Hugo: September 10–22, 1989. J. Coast. Res. Spec. Issue, 8: 163–179.

Penland, S., Suter, J.R., Sallenger, A.H., Williams, S.J., McBride, R.A., Westphal, K.E., Reimer, P.D. and Jaffe, B.E., 1989. Morphodynamic signature of the 1985 hurricane impacts on the northern Gulf of Mexico. Proc. Sixth. Symp. on Coastal and Ocean Management. Am. Soc. Civ. Eng., pp. 4220–4234.

Pierce, C.H., 1939. The meteorological history of the New England Hurricane of September 21, 1938. Mon. Weather Rev., 67(August): 237–285.

Pore, N.A. and Barrientos, C.S., 1976. Storm Surge, Mesa N.Y. Bight Atlas Mon. 6, N.Y. Sea Grant Institute, Albany, NY, 44 pp.

Powell, M.D., Dodge, P.P. and Black, M.L., 1991. The landfall of Hurricane Hugo in the Carolinas — Surface wind distribution. Weather Forecast., pp. 379–399.

Risnychok, N.T., 1990. Hurricane — A familiarization booklet. National Hurricane Center, NOAA, 30 pp.

SethuRaman, 1979. Atmospheric turbulence and storm surge due to Hurricane Belle (1976). Mon. Weather Rev., 107: 314–321.

Sheets, R.C., 1993. Personal communication, National Hurricane Center, 1320 South Dixie Highway, Coral Gables, FL 33146, USA.

Simpson, R.H. 1974. The hurricane disaster potential scale. Weatherwise, 27: 169–186.

Sparks, P.B., 1991. Wind conditions in Hurricane Hugo and their effect on buildings in South Carolina. In: C.W. Finkl and O.H. Pilkey (Editors), Impacts of Hurricane Hugo: September 10–22, 1989. J. Coast. Res. Spec. Issue, 8: 13–24.

Stauble, D.K., Seaburgh, W.C. and Hales, L.Z., 1991. Effects of Hurricane Hugo on the South Carolina coast. In: C.W. Finkl and O.H. Pilkey (Editors), Impacts of Hurricane Hugo: September 10–22, 1989. J. Coast. Res. Spec. Issue, 8: 129–162.

Thieler, E.R. and Young, R.S., 1991. Quantitative evaluation of coastal geomorphological changes in South Carolina after Hurricane Hugo. In: C.W. Finkl and O.H. Pilkey (Editors), Impacts of Hurricane Hugo: September 10–22, 1989. J. Coast. Res. Spec. Issue, 8: 187–200.